Electronic and structural properties of Cu-Au alloys

P. Weinberger, V. Drchal,* L. Szunyogh,† and J. Fritscher
Institut für Technische Elektrochemie, Technical University of Vienna, Getreidemarkt 9/158, A-1060 Vienna, Austria

B. I. Bennett
Los Alamos National Laboratory, Los Alamos, New Mexico 87545
(Received 24 November 1993)

The electronic and structural properties of random Cu-Au alloys have been determined using the (all-electron) fully relativistic Korringa-Kohn-Rostoker coherent potential approximation. The concentration was varied in steps of 10% (5% for the A_3B and AB_3 compositions) and total energy calculations were carried out to determine the corresponding equilibrium lattice constants. Just like the experimental data from which they differ at most by 1.5%, the calculated equilibrium lattice constants show a positive deviation from Vegard's law. The calculated heat of mixing agrees well with the existing experimental data. The equilibrium spectral properties of random Cu-Au alloys are discussed in terms of theoretical photoemission spectra and are compared to experimental data for Cu_3Au and pure Au. The structural properties of the compositional series are presented using lattice-constant- and concentration-dependent effective pair (and triplet) interactions up to fourth (tenth) -nearest neighbors and related quantities such as ordering energies and antiphase boundary energies. The ordering processes that govern the Cu_3Au and CuAu structure are discussed.

I. INTRODUCTION

There is an extensive history in modern times on the physics of the Cu-Au system. However, the alloy's phase diagram is still the subject of investigation by researchers. If one compares the phase diagram in Ref. 1 with more recent diagrams[2,3] one can see phase fields being revised or questioned. Much of the attention has been devoted to the study of the order-disorder phase transition in Cu_3Au, using experimental techniques such as diffuse electron scattering,[4,5] x-ray scattering,[3] extended x-ray-absorption fine structure (EXAFS),[6] or specific heat measurements.[7] These experiments have inspired a series of theoretical investigations that have become prominent in alloy theory[8] and have introduced metallurgical concepts such as antiphase domain boundaries.[9]

Most of the theoretical alloy papers in the sixties and seventies also dealt in one way or the other with the Cu-Au system. In the eighties special techniques such as neutron diffraction[10] or angle-resolved photoemission[11] were used to trace the critical temperature of the order-disorder phase transition in Cu_3Au by its characteristic features. Of course thermal analysis and other "classical" techniques were used much earlier to classify this system.[12,13]

With the establishment of (angle-integrated) valence-band photoemission spectroscopy as a standard experimental technique and the improvement in large-scale computational resources, theorists were prompted to attempt extensive electronic structure calculations to describe the alloy system's properties. There is a whole series of such calculations, roughly beginning with Ref. 14, that deal mostly with the ordered structure of Cu_3Au and sometimes with its disordered state. Ordered structures were also used, in terms of a Connolly-Williams-type approach, to describe phase stability and other thermodynamical properties of the Cu-Au alloys.

In this work a charge-self-consistent (all-electron) fully relativistic Korringa-Kohn-Rostoker coherent potential approximation (KKR-CPA) study (see, e.g., Ref. 15) is presented that covers a closely spaced range of alloy concentrations. The calculations show predicted equilibrium lattice constants, heats of mixing, theoretical (angle-integrated) photoemission intensities, and ordering energies and antiphase boundary energies based on effective pair interactions.

II. COMPUTATIONAL DETAILS

All calculations are based on the Gunnarson-Lundqvist exchange-correlation local-density functional[16] and were carried out using a maximum angular momentum quantum number of 3, the 21 special directions of Fehlner and Vosko[17] for the Brillouin zone integrations, and an energy mesh along the real energy axis corresponding to about 160–220 energy points in the valence region. For each self-consistent iteration the core charge density is recomputed. This procedure allows for the proper screening of the nuclear charge and the subsequent readjustment of the valence electrons. At each concentration, 4–7 different lattice constants were used to compute the total energy in order to locate its minimum value and, hence, determine the concentration's equilibrium lattice constant. For a particular lattice constant and concentration the alloy's total energy and the constituent total energies (see, e.g., Ref. 18) for Cu and Au were typically converged to considerably less than 0.5 mRy. In all calculations the same number of radial mesh points that define the charge

density were used and the muffin-tin radius corresponded to the inscribed Wigner-Seitz sphere.

After a calculation obtained a self-consistent charge density the off-diagonal scattering path operators, necessary to determine effective pair (and triplet) interactions (see, e.g., Ref. 19), were calculated using the Fehlner and Vosko directions.[17] Since an l-convergence study for the effective pair interactions showed little sensitivity with respect to an inclusion of the f channels, the effective pair interactions and related quantities presented in this paper are based on a maximum angular momentum quantum number of 2.

III. RESULTS

A. Equilibrium lattice constants and heat of mixing

Figure 1 shows the variation of the calculated equilibrium lattice constant as the concentration of Au (c_{Au}) is changed, along with the experimental data.[20] As can be seen from Fig. 1, in the range $0.3 < c_{\mathrm{Au}} < 0.75$ both the theoretical results and the experimental data give a positive deviation from Vegard's law. This deviation begins at about $c_{\mathrm{Au}} = 0.25$ and tends to return to the line depicting Vegard's law after $c_{\mathrm{Au}} = 0.75$. The largest deviation by the theory from the corresponding experimental values, about 1.5%, is in the region around $c_{\mathrm{Au}} \sim 0.5$.

As is well known, at $c_{\mathrm{Au}} \sim 0.3$ the long-period structures (Cu_3Au II structures) are expected,[20] while for $c_{\mathrm{Au}} \sim 0.7$ the experimental situation with respect to such long-period structures seems to be somewhat less clear. It will be shown in the Sec. III C that the alloy structure in the concentration range $0.3 < c_{\mathrm{Au}} < 0.75$ can be understood from the theory. The concentration ranges bounding this region will be seen to be related to ordering phenomena. It should be noted that for $c_{\mathrm{Au}} > 0.75$ and for $c_{\mathrm{Au}} < 0.3$ the calculated equilibrium lattice constants agree very well with the experimental data. In these two regimes of concentrations, the deviation from experiment is considerably less than 1%.

The heat of mixing is not only theoretically a very sensitive quantity, but also experimentally quite demanding. In Fig. 2 two experimental curves,[21] namely for "equilibrium samples" at 720 K and "quenched samples" at 320 K, are shown with respect to the concentration of Au, along with the theoretical values. As can be seen from the figure, the experimental curve for the quenched samples is lower than the one for the equilibrium samples and also much more symmetric around $c_{\mathrm{Au}} = 0.5$. Also there seems to be no shoulder at about $c_{\mathrm{Au}} = 0.25$ for the quenched samples as is seen for the equilibrium samples. For $c_{\mathrm{Au}} > 0.4$ the theoretical values are in good agreement with the experimental data for the equilibrium samples, while for $c_{\mathrm{Au}} < 0.4$ the theoretical values are in better agreement with the quenched samples. By inspecting the componentlike contributions to the heat of mixing, namely $c_\alpha(E^\alpha_{\mathrm{alloy}} - E^\alpha_{\mathrm{metal}})$ (see also Ref. 18), one discovers a kind of shoulder at $c_{\mathrm{Au}} \sim 0.25$ that reflects the corresponding behavior in the lattice constants (see Fig. 1) and which is not resolved in the sum over the components α. It should be noted, however, that since the total energy of Au is about one order of magnitude larger than that of Cu, even at low concentrations of Au the averaged total energy and, consequently, the heat of mixing is essentially determined by the numerical accuracy that can be achieved for the Au component total energy.

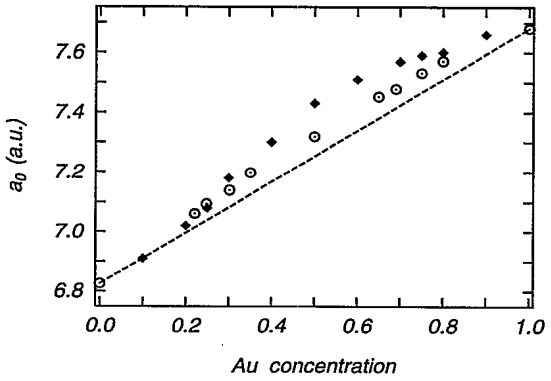

FIG. 1. Calculated (diamonds) and experimental (Ref. 20) (circles) equilibrium lattice constants for the system Cu_xAu_{1-x}. Vegard's law is indicated as a dashed line.

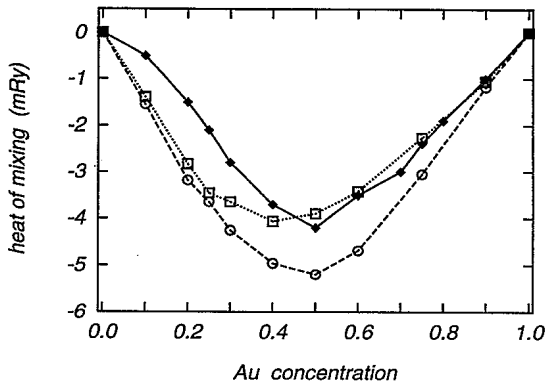

FIG. 2. Heat of mixing in $Cu_{1-x}Au_x$. The experimental values (Ref. 21) for the "equilibrium samples" (at 720 K) and the "quenched samples" (at 320 K) are indicated as squares and circles, respectively, and the theoretical values as diamonds.

B. Spectral properties

Figure 3 shows the calculated Al $K\alpha$ x-ray photoemission spectra (XPS) (see, e.g., Ref. 24 and references therein) for the whole series of concentrations investigated, along with a component decomposition for the Au_3Cu, AuCu, and $AuCu_3$ random alloys. All calculated spectra have an assumed total broadening function (lifetime broadening and spectrometer function) of 1 eV. Figure 4 shows the variation of the binding energies of the prominent peaks with respect to c_{Au}. Also marked in this figure are the experimental binding energies for Cu_3Au,[25] and pure Au.[26]

Like previous calculations[22,23] for Cu_3Au, the present

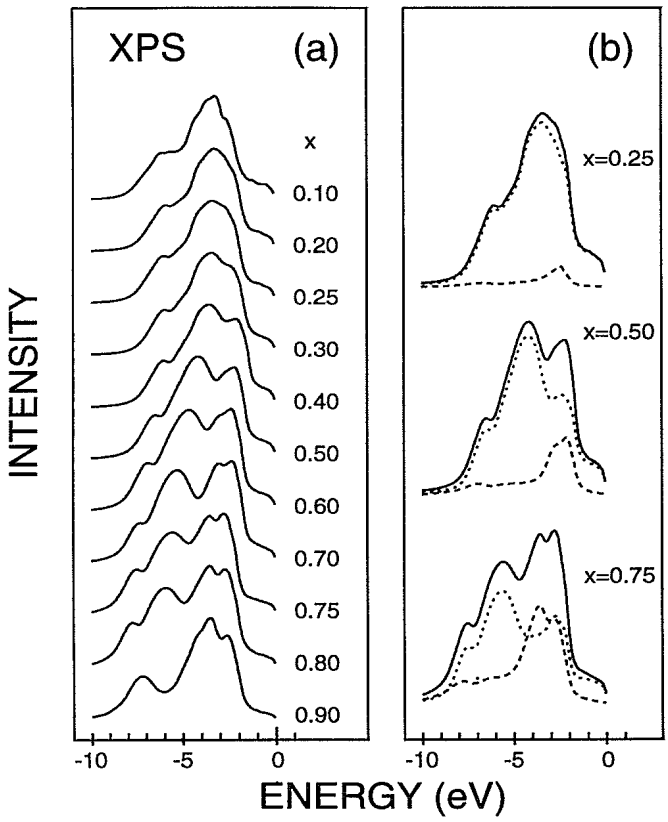

FIG. 3. (a) Theoretical Al $K\alpha$ photoemission spectra for $Cu_{1-x}Au_x$. (b) Decomposition of the Al $K\alpha$ photoemission spectra for $Cu_{75}Au_{25}$ (top), $Cu_{50}Au_{50}$ (middle), and $Cu_{25}Au_{75}$ (bottom) with respect to the components Cu (dashed line) and Au (dotted line).

calculation places the peak with the lowest binding energy about 0.6 eV too low in energy, while all other peaks seem to be in excellent agreement with experiment.[25] From Fig. 4 one can see that for $c_{Au} < 0.5$ the two lowest peaks move toward lower binding energy as the concentration of Au is decreased. They collapse into one

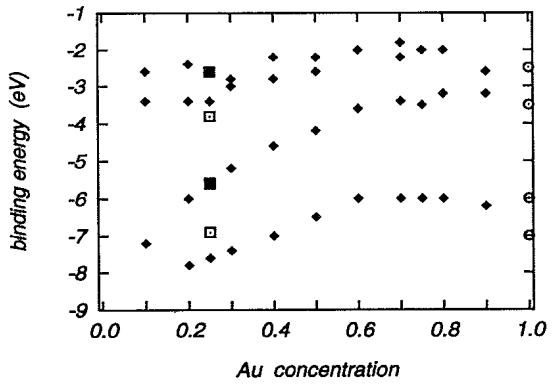

FIG. 4. Binding energies as a function of the concentration of Au. The theoretical values are shown as diamonds, and the experimental values for Cu_3Au and pure Au as squares and circles, respectively.

peak at $Cu_{90}Au_{10}$ and this peak moves up slightly in energy toward the value for the binding energy one expects to see in a corresponding experimental spectrum. The reasons for this obvious failure to describe the energetic position of this particular peak are not quite clear. Since the two lowest peaks in the $Cu_{75}Au_{25}$ spectrum correspond to the Au $d^{3/2}$- and the Au $d^{5/2}$-like contributions to the total spectrum, respectively, arguments based on missing Madelung terms[28] do not apply, since this effect would also shift the Au $d^{5/2}$-like peak toward higher binding energies, and that peak is already in good agreement with the experimental data. Of course the effect of displacive relaxations[29] due to size effects cannot be excluded, although from the shape of the effective scattering amplitudes and energetic position of the occurring resonances, this does not seem to be the case. It should be noted that the failure to describe the position of the Au $d^{3/2}$-like peaks is also a difficulty[30] in the ultraviolet photoemission regime. It is well known that the Cu-Au system shows surface segregation with an enhanced Au concentration near the surface.[31] It might very well turn out that in order to describe the photoemission from Cu_3Au surfaces properly, one has to incorporate a concentration gradient near the surface into the theoretical models, i.e., one has to deal with an inhomogeneous CPA problem and the problem of semi-infinite systems.[32] In principle, many-body effects could play a role in an explanation, although for the Au-Pd system[24] this did not seem to be the case.

From Fig. 4, one sees that for Au-rich alloys the energetic positions of the peaks faithfully reproduce the experimental binding energies[26] for pure Au, although the lowest peak usually only shows up in theoretical calculations for pure Au.[27] Figure 4 clearly indicates the need for a careful experimental photoemission study for the Cu-Au system, covering the whole range of concentrations by using a well-defined *in situ* cleavage technique and a suitable range of incident photon energies to sort out Cooper minima. For the time being, Figs. 3 and 4 represent the angle-integrated (valence-band) photoemission for the Cu-Au system.

C. Ordering energies and antiphase boundary energies

The purpose of this section is to interpret the parameters in an Ising Hamiltonian[33,34] for homogeneous alloys:

$$H = \frac{1}{2}\sum_{i,j} V_{ij}\delta c_i \delta c_j + \frac{1}{3}\sum_{ijk} V_{ijk}\delta c_i \delta c_j \delta c_k + \cdots \quad ,$$

where the V_{ij} and the V_{ijk} are effective pair and triplet interactions, respectively, and the δc_i's are the local concentration fluctuations, in terms of ground-state concepts such as ordering energies and antiphase boundary energies. In what follows, pair interactions are denoted simply by V_i, where i identifies the ith nearest neighbor.

In Fig. 5 the effective pair interactions up to the tenth-nearest neighbors are shown for $Cu_{25}Au_{75}$, $Cu_{50}Au_{50}$, and $Cu_{75}Au_{25}$ at a lattice constant closest to the calculated equilibrium lattice constant. The plots for

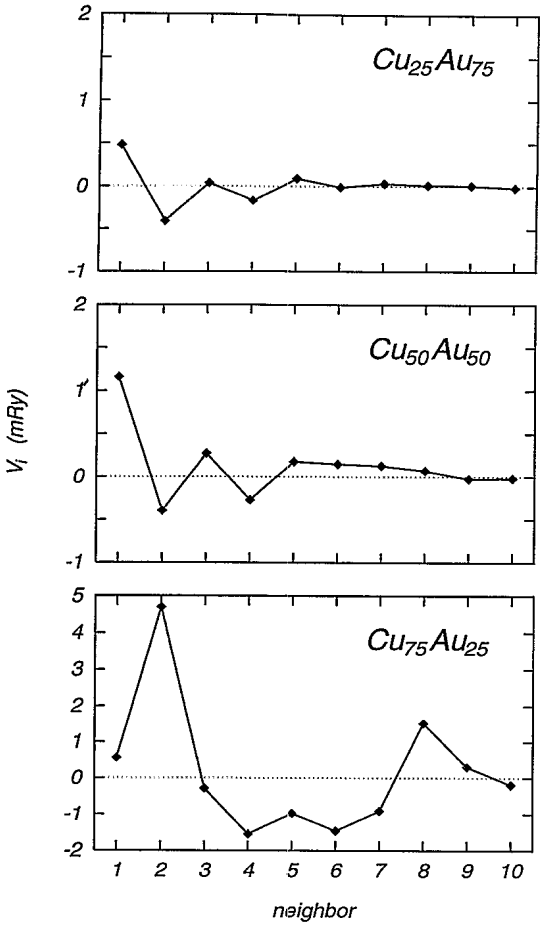

FIG. 5. Effective pair interactions for $Cu_{25}Au_{75}$ ($a = 7.60$ a.u., top), $Cu_{50}Au_{50}$ ($a = 7.45$ a.u., middle), and $Cu_{75}Au_{25}$ ($a = 7.075$ a.u., bottom) up to the tenth-nearest neighbors.

$Cu_{25}Au_{75}$ and $Cu_{50}Au_{50}$ seem to confirm the use of such pair interactions for the Cu-Au system in previous statistical mechanics calculations (for a review of parameters see, e.g., Ref. 35), namely $V_1, V_3 > 0$, $V_2, V_4 < 0$ with all higher pair interactions being quite small. For $Cu_{75}Au_{25}$ this obviously is not the case.

Table I shows the combinations of the first four effective pair interactions needed to calculate ordering energies (E_{ord}) for the possible ground-state structures appropriate for these alloy compositions.[36] Using these combinations and the antiphase boundary energy,[35] $E_{apb} = -V_2 + 4V_3 - 4V_4$, one obtains the lattice-constant-dependent quantities displayed in Fig. 6 for $Cu_{25}Au_{75}$, $Cu_{50}Au_{50}$, and $Cu_{75}Au_{25}$.

From Fig. 6 one can see that for $Cu_{50}Au_{50}$, E_{ord} and E_{apb} are weak functions of the lattice constant. The predicted ground-state structure for $Cu_{50}Au_{50}$ undoubtedly is the CuAu structure. The theoretical ordering energy of -1.43 mRy at the calculated equilibrium lattice constant (7.43 a.u.) for this structure is only about half of the experimental value of -2.93 mRy[21] for the equilibrium samples, but very close to the value for the quenched samples, namely -1.66 mRy. At the calculated equilibrium lattice constant, $E_{apb} = 2.3$ mRy.

For the $Cu_{25}Au_{75}$ system, the calculations predict quite a different behavior. In this case the system clearly orders as expected in the Cu_3Au structure and the theoretical ordering energy of -1.16 mRy at the calculated equilibrium lattice constant (7.59 a.u.) agrees fairly well with the corresponding experimental value of -0.65 mRy[21] for the equilibrium samples (0.16 mRy for the quenched samples). Under pressure (i.e., for smaller lat-

TABLE I. Ordering energies based on fourth-nearest-neighbor effective pair interactions.

Concentration	Structure	Ordering energy
0.5	CuAu	$-\frac{1}{2}V_1 + \frac{3}{4}V_2 - V_3 + \frac{3}{2}V_4$
	CuPt	$-\frac{3}{4}V_2 + \frac{3}{2}V_4$
	AB_{-40}	$-\frac{1}{2}V_1 + \frac{1}{4}V_2 + V_3 - \frac{1}{2}V_4$
0.25, 0.75	Cu_3Au	$-\frac{3}{8}V_1 + \frac{9}{16}V_2 - \frac{3}{4}V_3 + \frac{9}{8}V_4$
	DO_{22}	$-\frac{5}{8}V_1 + \frac{5}{16}V_2 + \frac{1}{4}V_3 + \frac{1}{8}V_4$
	DO_{23}	$-\frac{5}{8}V_1 + \frac{7}{16}V_2 - \frac{1}{4}V_3 + \frac{5}{8}V_4$

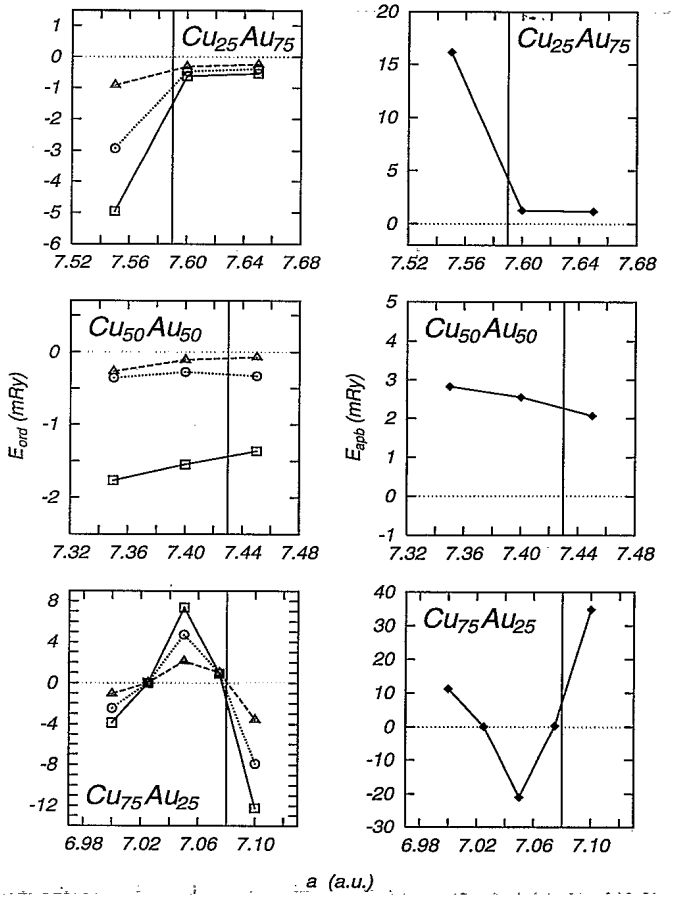

FIG. 6. Ordering energies (left) and antiphase boundary energy (right) for $Cu_{25}Au_{75}$ (top), $Cu_{50}Au_{50}$ (middle), and $Cu_{75}Au_{25}$ (bottom). The equilibrium lattice constants are indicated by vertical lines. For the A_3B and AB_3 compositions the Cu_3Au, DO_{22}, and DO_{23} ordering energies are shown as squares, triangles, and circles, respectively. For the AB composition the CuAu, CuPt, and AB_{40} ordering energies correspond to squares, triangles, and circles, respectively.

tice constants), the system exhibits a substantial decrease in the ordering energy with an attendant increase in the antiphase boundary energy.

For the $Cu_{75}Au_{25}$ system the ordering energies for the Cu_3Au, DO_{22}, and DO_{23} structures as well as the antiphase boundary energy are strongly dependent on the lattice constant. At the calculated equilibrium lattice constant of 7.08 a.u., which agrees very well with the corresponding experimental value, the theoretical Cu_3Au ordering energy of -2.0 mRy is almost identical with the value obtained experimentally (-2.04 mRy for the equilibrium samples and -2.08 mRy for the quenched samples[21]). Inspecting Fig. 6, however, one has to admit that this kind of agreement is probably coincidental rather than a clear confirmation of the experimental data, since for lattice constants only marginally smaller than the equilibrium lattice constant all three ordering energies become positive. At 7.05 a.u. the ordering energy for the DO_{22} structure is lower than those for the Cu_3Au and DO_{23} structures. From Fig. 5 one can see that for $Cu_{75}Au_{25}$ the energy expansion using (effective) pair interactions cannot be restricted to only fourth-nearest neighbors: higher pair interactions can contribute substantially to the ordering energy. Figure 6 also clearly shows that the antiphase boundary energy is strongly dependent on the lattice constant and that near the equilibrium lattice constant E_{apb} is nearly zero.

As already mentioned before in the context of Fig. 1, at $c_{\mathrm{Au}} = 0.25$ one sees the onset of a strong deviation from Vegard's law toward larger lattice constants. Upon reaching $c_{\mathrm{Au}} = 0.75$, one can see a tendency to return to smaller lattice constants, eventually reaching the value appropriate for pure Au. Returning to Fig. 6, one sees that for $Cu_{25}Au_{75}$ the system can gain ordering energy by moving to smaller (averaged) lattice spacings, while for $Cu_{75}Au_{25}$ the opposite is true. Based on this reasoning, it seems quite likely that displacement fluctuations play a decisive role in the ordering of the Cu_3Au structure (an interesting discussion thereof is given in Ref. 37).

As far as the range of concentrations $0.3 \leq c_{\mathrm{Au}} \leq 0.6$ is concerned, from Fig. 7 one sees that the effective pair interactions are only weakly dependent on concentration and lattice constant. On the other hand, perhaps $Cu_{70}Au_{30}$ can be regarded as a kind of precursor for $Cu_{75}Au_{25}$, since V_1 shows a minimum near the calculated equilibrium lattice constant of 7.18 a.u. In this regime of concentrations the antiphase boundary energy is positive and varies only very little with the lattice spacing. A special case is $Cu_{30}Au_{70}$ for which, at the calculated equilibrium lattice constant (7.57 a.u.), the antiphase boundary energy is very nearly zero, possibly an indication for the occurrence of long-period structures in the vicinity of $c_{\mathrm{Au}} = 0.75$.

Figure 8 shows the effective pair interactions for the alloys $Cu_{90}Au_{10}$ and $Cu_{10}Au_{90}$. The effective pair interactions are rather large and strongly lattice-constant dependent. For these two concentrations effective triplet interactions become important, which are in turn strongly lattice-constant dependent.

For $0.4 \leq c_{\mathrm{Au}} \leq 0.7$ the triplet interactions V_{012}, V_{013}, V_{014}, and V_{024} (for a definition in terms of spanning vec-

TABLE II. Spanning vectors for effective triplets.

V_{ijk}	$\vec{R}_i$	$\vec{R}_j$	$\vec{R}_k$
V_{012}	$(0,0,0)$	$(\frac{1}{2},\frac{1}{2},0)$	$(1,0,0)$
V_{013}	$(0,0,0)$	$(\frac{1}{2},\frac{1}{2},0)$	$(1,\frac{1}{2},\frac{1}{2})$
V_{014}	$(0,0,0)$	$(\frac{1}{2},\frac{1}{2},0)$	$(1,1,0)$
V_{024}	$(0,0,0)$	$(1,0,0)$	$(1,1,0)$

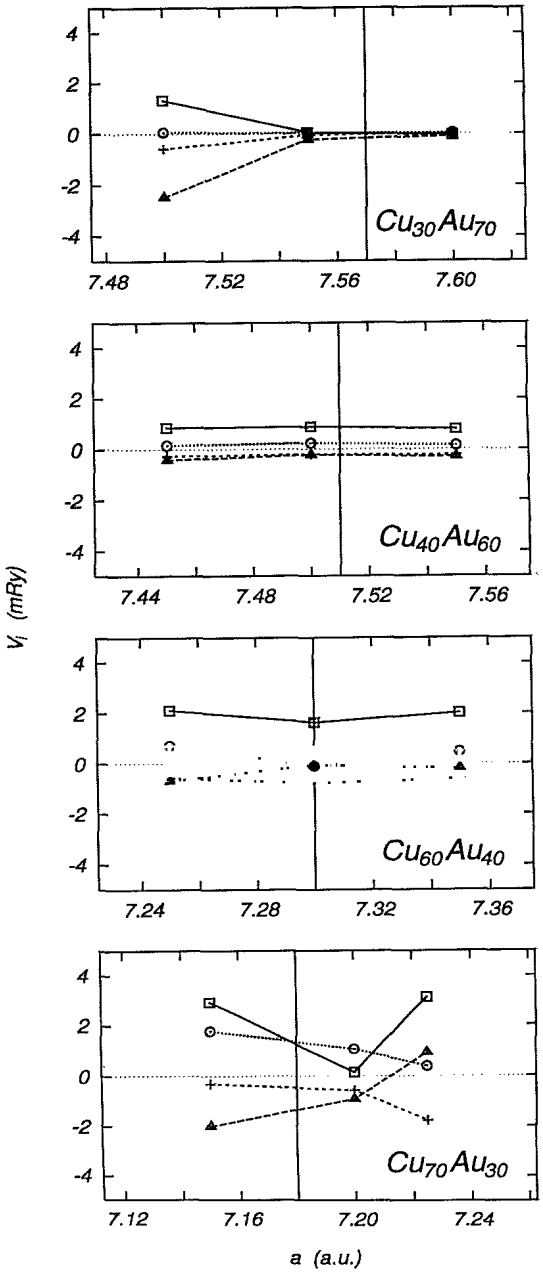

FIG. 7. First four effective pair interactions for $Cu_{30}Au_{70}$, $Cu_{40}Au_{60}$, $Cu_{60}Au_{40}$, and $Cu_{70}Au_{30}$. V_1, V_2, V_3, and V_4 are shown as squares, triangles, circles, and pluses, respectively. The equilibrium lattice constants are indicated by vertical lines.

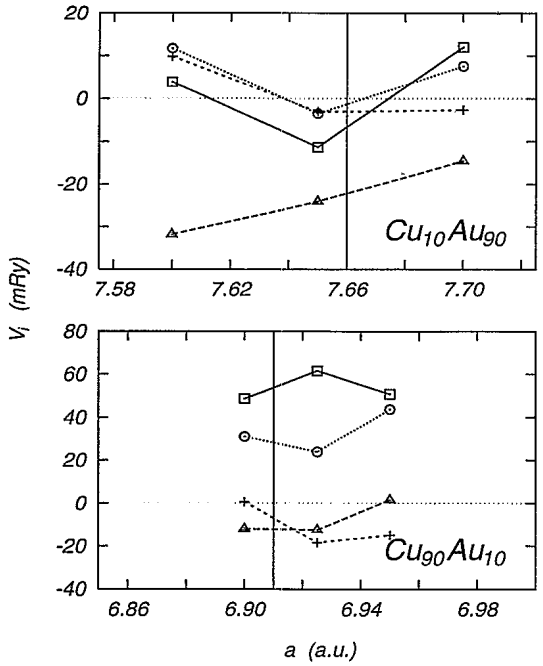

FIG. 8. First four effective pair interactions for $Cu_{90}Au_{10}$ and $Cu_{10}Au_{90}$. V_1, V_2, V_3, and V_4 are shown as squares, triangles, circles, and pluses, respectively. The equilibrium lattice constants are indicated by vertical lines.

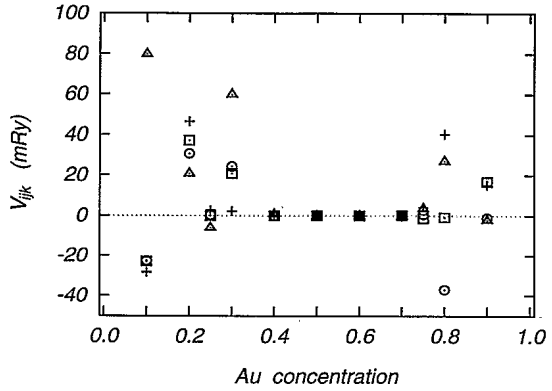

FIG. 9. Effective triplet interactions for Cu_xAu_{1-x} at the respective equilibrium lattice constant as a function of the concentration of Au. V_{012}, V_{013}, V_{014}, and V_{024} are shown as squares, triangles, circles, and pluses, respectively.

tors in real space, see Table II) are typically one order of magnitude smaller than the corresponding pair interactions. In Fig. 9 these four triplet interactions are displayed versus the concentration of Au at their respective equilibrium lattice constants. Typically it seems to be the case that whenever the pair interactions are large then the triplet interactions also become large. There is one important exception, namely $Cu_{70}Au_{30}$, for which the triplet interactions are large and the pair interactions rather small. It should be recalled that near $c_{Au} \sim 0.3$ the Cu_3Au II structures have to be expected. It is difficult to decide whether or not the behavior of the triplet interactions is an indication for invoking the concept of concentration-independent pair interactions proposed by Wolverton *et al.*[38] or simply related to the occurrence of the Cu_3Au structure and/or displacement fluctuations. At present, no simple models of interpretation of triplet interactions in terms of energy concepts are available.

IV. SUMMARY

The present charge-self-consistent fully relativistic KKR-CPA calculations give a reasonably good account of the observed equilibrium lattice constants, of the heat of mixing, and of the ordering energies into the CuAu or Cu_3Au structures. From the discussion of the pair interactions and ordering energies, it seems that for the Cu-Au system the basic underlying structure is the CuAu structure, whereas the formation of the Cu_3Au structure requires both ordering effects with respect to the parent fcc lattice and displacement fluctuations. In order to rule out ambiguities with respect to triplet and higher-order interactions, statistical mechanics calculations have to be performed based on the present pair interactions and on the use of integrated densities of states corresponding to defined configurations in a first-nearest-neighbor cluster as a pickup table for Monte Carlo calculations.[39] It should be noted, however, that when using the embedded cluster method[40] in this way,[41] one has to deal in principle with 144 configurations per component. Such calculations are presently under preparation. The calculated x-ray photoemission spectra showed a consistent shift of peaks with respect to the concentration, which seems to yield correct binding energies for Au-rich alloys, but fails to give a good account of the lowest peak in Cu_3Au —at least with respect to the existing experimental data.

ACKNOWLEDGMENTS

All calculations were performed using the parallel virtual machine (PVM) software either on a four-processor Cray XMP or on clusters of IBM RISC workstations. Financial support from the Austrian Nationalbank (Project No. 4648), the Austrian Ministry of Science (Project No. GZ 49.731/2-24/91), and the Austrian Science Foundation (Project No. P7996) is gratefully acknowledged. Also appreciated is the assistance provided by the Computing and Communications Division and the Superconductivity Technology Center at the Los Alamos National Laboratory.

*On leave from Institute of Physics, Academy of Sciences of the Czech Republic, CZ-180 40 Praha 8, Czech Republic.
†On leave from Physical Institute, Technical University Budapest, Budafoki út. 8, H-1111 Budapest, Hungary.

[1] M. Hansen, *Constitution of Binary Alloys* (McGraw-Hill, New York, 1958).
[2] M. Guymont, R. Portier, and D. Gratias, as cited in F. Ducastelle, *Order and Phase Stability in Alloys* (North-

Holland, Amsterdam, 1991).
[3]M. Bessière, S. Lefebvre, and Y. Calvayrac, Acta Crystallogr. Sect. B **39**, 145 (1983).
[4]D. Watanabe and P. M. J. Fisher, J. Phys. Soc. Jpn. **20**, 2170 (1965).
[5]S. Hashimoto and S. Ogawa, J. Phys. Soc. Jpn. **29**, 710 (1970); S. Hashimoto, Acta Crystallogr. Sect. A **30**, 792 (1974).
[6]T. Claeson and J. B. Boyce, Phys. Rev. B **29**, 1551 (1984).
[7]D. L. Martin, Phys. Rev. B **14**, 369 (1976).
[8]P. C. Clapp and S. C. Moss, Phys. Rev. B **171**, 764 (1968); J. Appl. Crystallogr. **8**, 96 (1974); S. C. Moss, Phys. Rev. Lett. **22**, 1108 (1969); S. C. Moss and R. H. Walker, J. Appl. Crystallogr. **8**, 96 (1974).
[9]J. Zhu and J. M. Cowley, Acta Crystallogr. Sect. A **38**, 718 (1982).
[10]G. H. Lander and P. J. Brown, J. Phys. C **18**, 2017 (1985).
[11]R. G. Jordan, G. S. Sohal, B. L. Gyorffy, P. J. Durham, W. M. Temmerman, and P. Weinberger, J. Phys. F **15**, L135 (1985).
[12]W. C. Roberts-Austen and T. K. Rose, Proc. R. Soc. London, Ser. A **67**, 105 (1900).
[13]L. Vegard and H. Dale, Z. Kristallogr. **67**, 157 (1928).
[14]H. L. Skriver and H. P. Lengkeek, Phys. Rev. B **19**, 900 (1979).
[15]P. Weinberger, *Electron Scattering Theory for Ordered and Disordered Matter* (Clarendon, Oxford, 1990).
[16]O. Gunnarsson and B. I. Lundqvist, Phys. Rev. B **13**, 4274 (1976).
[17]W. R. Fehlner and S. H. Vosko, Can. J. Phys. **54**, 2159 (1976).
[18]P. Weinberger, J. Kudrnovský, J. Redinger, B. I. Bennett, and A. M. Boring, Phys. Rev. B **48**, 7866 (1993).
[19]P. Weinberger, C. Blaas, B. I. Bennett, and A. M. Boring, Phys. Rev. B **47**, 10 158 (1993).
[20]W. B. Pearson, *Lattice Spacings and Structures of Metals and Alloys* (Pergamon, London, 1958).
[21]R. L. Orr, Acta Metall. **8**, 489 (1960).
[22]B. Ginatempo and J. B. Staunton, J. Phys. F **18**, 1827 (1988); P. Weinberger, A. M. Boring, R. C. Albers, and W. M. Temmerman, Phys. Rev. B **38**, 5357 (1988); E. Arola, R. S. Rao, A. Salokatve, and A. Bansil, *ibid.* **41**, 7361 (1990).
[23]V. Drchal, J. Kudrnovský, and P. Weinberger (unpublished).
[24]P. Weinberger, L. Szunyogh, and B. I. Bennett, Phys. Rev. B **47**, 10 154 (1993).
[25]V. V. Nemoshkalenko, K. V. Chuistov, V. G. Aleshin, and A. I. Senkevich, J. Electron Spectrosc. Relat. Phenom. **9**, 169 (1976); W. Eberhardt, S. C. Wu, R. Garrett, D. Sondericker, and F. Jona, Phys. Rev. B **31**, 8285 (1985); S. B. DiCenzo, P. H. Citrin, E. H. Hartford, Jr., and G. K. Wertheim, *ibid.* **34**, 1343 (1986).
[26]P. H. Citrin, G. K. Wertheim, and Y. Baer, Phys. Rev. B **27**, 3160 (1983); G. K. Wertheim and D. N. E. Buchanan, *ibid.* **3**, 914 (1986); R. I. R. Blyth, A. B. Andrews, A. J. Arko, P. C. Canfield, B. I. Bennett, and P. Weinberger (unpublished).
[27]U. König, P. Marksteiner, J. Redinger, P. Weinberger, and H. Ebert, Z. Phys. B **65**, 139 (1986).
[28]R. Magri, S.-H. Wei, and A. Zunger, Phys. Rev. B 42, 11 388 (1990).
[29]Z. W. Lu, S.-H. Wei, and A. Zunger, Phys. Rev. B **45**, 10 314 (1992).
[30]B. Ginatempo, P. J. Durham, and B. L. Gyorffy, J. Phys. Condens. Matter **1**, 6483 (1989); B. Ginatempo, B. L. Gyorffy, and G. M. Stocks, in *Metallic Alloys: Experimental and Theoretical Perspectives*, Vol. 256 of *NATO Advanced Study Institute, Series E: Applied Sciences*, edited by S. L. Faulkner and R. G. Jordan (Kluwer Academic, Dordrecht, 1994), p. 55.
[31]V. Kumar and K. H. Bennemann, Phys. Rev. Lett. **53**, 278 (1984), and references therein.
[32]A. Pasturel, V. Drchal, J. Kudrnovský, and P. Weinberger, Phys. Rev. B **48**, 2704 (1993); J. Kudrnovský, I. Turek, V. Drchal, P. Weinberger, S. K. Bose, and A. Pasturel, *ibid.* **47**, 16 525 (1993).
[33]A. Gonis, X.-G. Zhang, A. J. Freeman, P. E. A. Turchi, G. M. Stocks, and D. M. Nicholson, Phys. Rev. B **36**, 4630 (1987).
[34]J. Klíma, Z. Phys. B **90**, 267 (1993).
[35]F. Ducastelle, *Order and Phase Stability in Alloys* (Ref. 2).
[36]M. Sluiter and P. E. A. Turchi, Phys. Rev. B **40**, 11 215 (1989).
[37]B. Chakraborty, in *Metallic Alloys: Experimental and Theoretical Perspectives* (Ref. 30), p. 241.
[38]C. Wolverton, M. Asta, H. Dreyssé, and D. de Fontaine, Phys. Rev. B **44**, 4914 (1991); C. Wolverton, G. Ceder, D. de Fontaine, and H. Dreyssé, *ibid.* **48**, 726 (1993).
[39]Y. Wang, S. L. Faulkner, and G. M. Stocks, Phys. Rev. Lett. **70**, 3287 (1993).
[40]A. Gonis, W. H. Butler, and G. M. Stocks, Phys. Rev. Lett. **50**, 1482 (1983); A. Gonis, G. M. Stocks, W. H. Butler, and H. Winter, Phys. Rev. B **29**, 555 (1984).
[41]J. Banhart, P. Weinberger, and J. Voitländer, Phys. Rev. B **40**, 12079 (1989).